

# Mathematical Modelling of Formation Heat Treatment Process

A. K. M. JAMALUDDIN\* and C. T. BOWEN

Noranda Technology Centre, 240 Hymus Blvd., Pointe Claire, QC H9R 1G5, Canada

and

M. HASAN

Department of Mining and Metallurgical Engineering, University of McGill, 3450 University Street, Montreal, QC H3A 2A7, Canada

A novel matrix stimulation concept, formation heat treatment (FHT), which involves the application of intense heat around the near-wellbore region for the treatment of water blockage and clay related formation damage in water sensitive formations previously was developed and presented in the literature. The FHT process involves the application of intense heat around the wellbore using a downhole heater. The heat is conveyed to the near-wellbore region using an inert gas flowing through a downhole heater.

To understand the heat transfer and fluid-flow characteristics of the FHT process, a transient two-dimensional mathematical model has been developed and is presented in this paper. The model is based on coupling the momentum and energy-balance equations for the wellbore gas with the surrounding porous formation. The presence of the heater across the net pay (sandface) is taken into account in the energy equation as a localized volumetric heat source. A control-volume based finite-difference scheme is used to solve the model equations on a staggered grid. Parametric studies indicate that by injecting a suitable quantity of gas through the tube and annulus, and by adjusting the power input to the downhole heater, the temperature near the wellbore can be favourably controlled.

On a mis au point et présenté antérieurement dans la littérature scientifique un nouveau modèle de simulation matricielle pour le traitement de chaleur de formation (FHT), basé sur l'application d'une chaleur intense autour de la région du puits de forage pour le traitement du blocage des pores et des dommages à la formation liés à l'argile dans les formations sensibles à l'eau. Le procédé FHT utilise pour ce faire une chaudière à orifice descendant. La chaleur est conduite à la région du puits à l'aide d'un écoulement de gaz inerte dans la chaudière à orifice descendant.

Afin de comprendre les caractéristiques du transfert de chaleur et de l'écoulement des fluides du procédé FHT, on a mis au point un modèle mathématique transitoire bidimensionnel. Ce modèle s'appuie sur le couplage des équations d'équilibre de conservation de la quantité de mouvement et d'énergie pour le gaz du puits de forage avec la formation poreuse environnante. La présence de la chaudière dans la production nette (côté sable) est prise en compte dans l'équation d'énergie comme source de chaleur volumétrique localisée. On utilise un schéma de différences finies basé sur les volumes de contrôle à grille décalée. Les études paramétriques indiquent qu'en injectant une quantité adéquate de gaz dans le tube et l'espace annulaire, et en ajustant la puissance dans la chaudière à orifice descendant, on peut contrôler favorablement la température près du puits de forage.

Keywords: wellbore damage, clay swelling, water blocking, formation heat treatment, simulation, temperature profile.

Petroleum engineering operations such as drilling, completion, workovers, and stimulation, expose the formation to a foreign fluid. This exposure results in fluid invasion into the near wellbore region. The permeability of the fluid invaded porous zone is reduced because of pore throat constriction caused by clay swelling, clay migration and water blocking. This fluid-invaded region with reduced permeability is called the "damaged zone," extending roughly 1 m into the reservoir. Clay-related formation damage during drilling and completion has long been identified to be a major problem. Measures to stabilize clay swelling and migration have been discussed in the literature (Himes et al., 1991; Borchardt et al., 1984; Theng, 1984; Reed, 1974; Coppell et al., 1973; Plummer, 1991). Curative methods have also been attempted and presented in the literature (Hayatdavoudi et al., 1992; Lund et al., 1976; Thomas and

Crowe, 1981; Garst, 1957; Sloat, 1989; Schaible, 1986; Crowe, 1986). The two most popular non-thermal stimulation processes are hydraulic fracturing and matrix acidizing.

One of the earliest reports of *in situ* thermal treatment was that of Albaugh (1954), on a field test that was carried out in an oil well in California. Since then, many other curative thermal processes have been described for a variety of purposes, including the removal of wax (Nenniger, 1992) or asphaltene (Winckler and McManus, 1990) buildups, thermal fracturing of the formation (White and Mass, 1965), and the consolidation of unconsolidated formations (Friedman et al., 1988). More specifically related to clay damage are methods aimed at evaporating blocked water (Reed, 1991a,b), dehydrating bound water from clays (White and Mass, 1965; Braun, 1971), or transforming a sensitive type of clay (e.g. smectite) into a less sensitive type (e.g. illite) (Carroll, 1970; Nooner, 1980).

A new matrix stimulation concept, called formation heat treatment (FHT), was tested in the laboratory and in the field (Jamaluddin and Nazarko, 1994; Jamaluddin et al., 1995, 1996a). The FHT process involves the application of heat for

\*Author to whom correspondence should be addressed. Present address: Hycal Energy Research Laboratories Ltd., 1338A - 36th Avenue N.E., Calgary, Alberta, Canada T2E 6T6.

the treatment of near wellbore damage. The heating around the wellbore is achieved using a downhole heater (Jamaluddin et al., 1996b) located at the sandface. The heat is conveyed from the heater to the near wellbore region by an inert gas (e.g. nitrogen) flowing through and around the heater.

To understand the heat transfer and fluid flow characteristics of downhole heating, various modelling efforts have been presented in the literature. A one-dimensional mathematical model (Sharma et al., 1989) was described for predicting the flowing temperature profile in a well with a downhole heater. The model was identical to Ramey's (1962) model, except that the heater was included through the treatment of a source term in the one-dimensional heat balance equation. Another mathematical model to calculate heat losses to the surrounding formations due to the downward injection of hot fluid through the tubing was presented by Hoang (1980) and referenced by Somerton (1992). The model divided the wellbore and its surroundings into two regions: tubing and formation. Hoang assumed that the heated fluid flowing through the tubing was losing heat radially to the surroundings, while in the formation heat was assumed to be conducted both radially and vertically. The analysis did not take into account any penetration of the hot fluid into the formation. Hoang's analysis showed that for an injection rate of 30,000 kg/h of the hot fluid, temperature profiles within the entire length of the tubing and surrounding formations reached a steady state within a few hours. He concluded that for a high injection rate of the hot fluid through the tubing, a transient analysis of the model equations was not necessary.

None of these studies coupled heat transfer and fluid flow phenomena for the injection of a gas in a wellbore where the gas was heated while passing through a downhole heater. All prior studies in this area were variations of Ramey's (1962) original work, where the fluid momentum equation was completely ignored. Furthermore, almost all studies in this area have combined the steady-state heat conduction solution for the wellbore with the approximate and unsteady-state heat conduction solution for the surrounding rock.

In this study, a two-dimensional mathematical model has been developed for the simulation of localized wellbore heating using nitrogen gas as the injection fluid. The presence of a downhole heater has been accounted for by incorporating a volumetric heat source term in the transient energy equation. The model uses two-dimensional axisymmetric turbulent Navier-Stokes equations and energy equations. Specifically, the model deals with the electrical heating of the nitrogen gas near the formation and predicts the flow fields and convective and conductive heat transfer characteristics between the heated gas and the surrounding reservoir. The model can be used to quantify the power requirement of the downhole heater and the heat propagation in the near wellbore region during the formation heat treatment process. In addition, the model allows for the optimization of the operating parameters.

#### Formation heat treatment (FHT) process logistics

The formation heat treatment (FHT) process consists of exposing the formation to an elevated temperature to cause:

- vaporization of blocked water,
- dehydration of the clay structure,
- partial destruction of the clay minerals, and
- possibly, micro-fracture of the formation in the near-wellbore area due to thermally induced stresses.

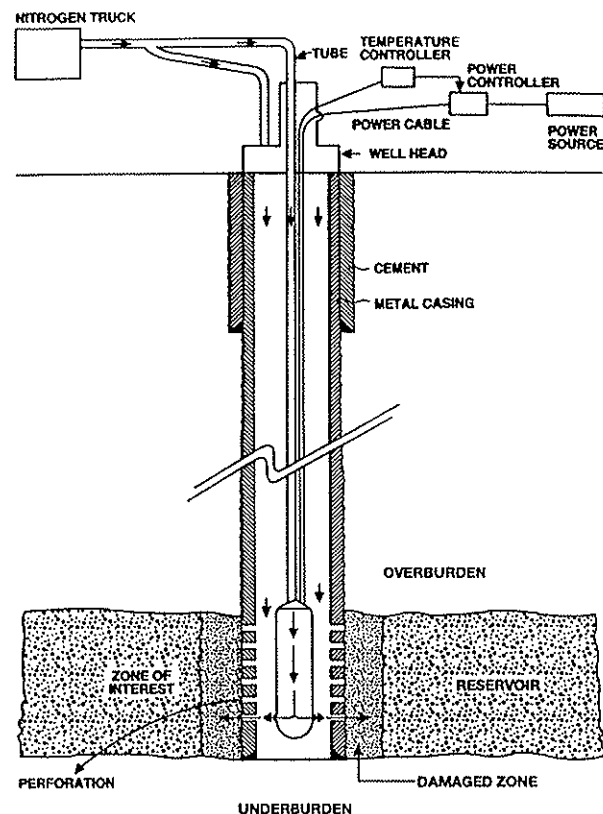


Figure 1 — Schematic diagram of the formation heat treatment (FHT) process logistics.

A series of bench scale heating tests was carried out on sandstone cores taken from both oil- and gas-bearing formations (Jamaluddin et al., 1995). Sample cores taken from actual formation displayed an 84% reduction in permeability following water exposure. Heating to a temperature around 400°C re-established the baseline permeability of the core. Further heating at 600 and 800°C improved the permeability to 50% and 760% above the baseline value, respectively.

The physical situation and field logistics of the formation heat treatment process are presented schematically in Figure 1. As seen in the figure, a downhole heater is attached to the end of a tubing and placed across the sandface. After lowering the tool, nitrogen gas is injected through both the tubing and the casing tubing annulus from the surface. The well is pressurized to a pressure higher than the corresponding reservoir pressure forcing the nitrogen into the reservoir. After pressurization, the tool is powered up to heat the injection nitrogen while it is flowing through the downhole heater and convey the heat to the near wellbore region of the reservoir.

The primary objective of the FHT process is the intense heating of the near wellbore region extending to 1 m radially in the reservoir. The duration of the total heating period is designed to be 6 to 8 hours. The heating period starts with a slow power up sequence and continues with a one hour heating period to establish steady state conditions after reaching the target temperature of the gas exiting the downhole heater.

To validate the field logistics and design, a multi-chamber, multi-pass, 60 kW electrical resistance type heating system was designed (Jamaluddin et al., 1996b), constructed, and tested. Due to voltage losses in the cable and limited space within the wellbore, the heater was restricted to 60 kW. The

current rating limited the operating power to 55 kW. Since the power was limited, the desired temperature had to be achieved by varying the total nitrogen flow rate. Based on the bench-scale results, the preferred temperature in the near-wellbore region was considered to be 800°C. To achieve this temperature in the formation, a higher temperature was required at the exit of the downhole heater. Due to power limitations and practical concerns of the effect of high temperature on casing and cement, the target temperature of the exit gas was set at around 700 to 800°C. The purpose of this simulation study was to identify the depth of heat penetration and to determine the temperature profile in the near wellbore region given the fixed power constraints.

### Model development

In this model, the vertical height of the well is divided into two segments: an upper segment and a lower segment. In the upper segment, the injected gas is assumed to enter the top of the well at a fixed volumetric flow at an atmospheric pressure and at a fixed injection pressure. A preset fraction of the injection volume is assumed to flow down the tubing and the remaining fraction of the total volume of the gas is assumed to flow through the tubing-casing annulus. Typically, 90% by volume is pumped through the tubing and 10% by volume through the casing-tubing annulus. The temperature of the gas in this upper vertical segment of the well is assumed to be in thermal equilibrium with the geothermal temperature. No account is made of the heat loss or heat gain in this region from the surroundings. The pressure profiles for the tubing and tubing-casing annulus for this upper vertical segment of the well are obtained after integrating the differential mechanical-energy balance equation and assuming that an average geothermal temperature prevails in this section. Since this study is concerned with the mass, momentum and heat transfer in the near wellbore with a heater near the bottomhole, the detailed mass, momentum and heat transfer analyses for the upper segment have not been carried out. It was verified through the preliminary analysis that the downstream results did not have any impact on the upstream calculations.

The target reservoir and the associated overburden and underburden regions constitute the domain of the FHT model (Figure 2). The FHT model domain is set at 20 m high ( $XL = 20$  m) and 10 m in diameter ( $YL = 5$  m). Out of the 20 m, the bottom 5 m is the net pay ( $h = 5$  m) and the remaining 15 m is overburden. A 4 m long downhole heater is positioned across the net pay (Figure 2). The first 1 m of the heater is a cold section where junction box and cooling chamber are housed (Jamaluddin et al., 1996b). The subsequent 3 m length is the hot region and the hot gas exit at the bottom of the heater (0.3 m opening). In the model, the outer diameter of the tool and the internal diameter of the casing is set to be 0.09 and 0.11 m ( $d_{ci} = 0.11$  m), respectively. The casing and cement across the net pay are perforated. The majority of the nitrogen (90%) is injected through the tubing and the remaining (10%) is injected through the casing-tubing annulus. The purpose of this annular injection is to reduce heat propagation upwards through the annular space.

The model domain (Figure 2) consists of five concentric zones in the radial direction across the net pay and four concentric zones in the overburden region. The five radial zones at the sandface are: tubing, casing-tubing annulus with perforated casing, perforated cement region outside the casing,

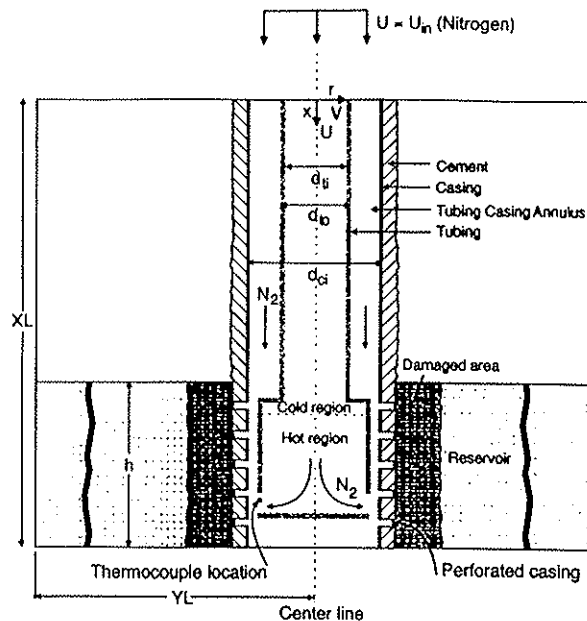


Figure 2 — Schematic diagram of the model domain.

damaged formation region, and part of the formation. The four concentric zones in the overburden are: tubing, casing-tubing annulus with unperforated casing, unperforated cement region, and impervious overburden. The near-wellbore region and the formation are bounded at the bottom by an impervious underburden.

Velocity, pressure, density of the injection gas and the geothermal temperature at the lowest end of the upper segment make up the input of the lower segment of the model region. In view of the complexity of the computational domain, the turbulent conditions (due to high injection rates) in the energy and momentum equations is modelled using the *ad-hoc* viscosity approach (Mishima and Szekely, 1989; Chan et al., 1991), where the thermal conductivity and viscosity of the gas is increased by factors of 100.

### UPPER SEGMENT OF THE WELLBORE

The flowing pressures in the tubing and tubing-casing annulus for upper segment were estimated using Equation (1) (Beggs, 1984; Carcoana, 1992), which is derived from the average pressure and temperature method. This calculation provided the input parameters for the lower segment.

$$P_{wf}^2 = P_{if}^2 e^s + 25 \gamma_g q^2 T_{ag} Z f H (e^s - 1) / S d^5 \dots \dots \dots (1)$$

In Equation (1),  $P_{wf}$  is the pressure in the tubing or annulus,  $P_{if}$  is the pressure at the inlet of the tube or annulus,  $H$  is the total height of the tube,  $T_{ag}$  is the average geothermal temperature,  $q$  is the total volumetric gas flow rate through the tube or annulus,  $d$  is the diameter of the tube or the equivalent diameter of the annulus,  $f$  is the turbulent friction factor and is calculated using Equation (2); parameter  $S$  is calculated using Equation (3).

$$f = 1.0 / [1.14 - 2.0 \times \log (\epsilon / d + 21.25 / Re^{0.9})]^2 \dots \dots \dots (2)$$

In Equation (2),  $\epsilon$  is the roughness of the tube or the tubing-casing annulus,  $Re$  is the Reynolds number for the tube or annulus.

$$S = 0.0375 \gamma_g H/T_{ag} Z \dots \dots \dots (3)$$

In Equations (1) and (3),  $\gamma_g$  is the specific gravity of the gas, and  $Z$  is the gas compressibility factor evaluated at  $T_{ag}$ .

LOWER SEGMENT OF THE WELLBORE (DOMAIN MODELLED)

The lower segment of the wellbore is considered to be the FHT model domain. Model regions are considered to be as presented in Figure 2. The coordinate system as well as various geometrical parameters also are presented in Figure 2. The nitrogen gas with constant physical properties enters the tube and annulus at a uniform (but not necessarily the same) velocity. Prior to the start of heating, the fluid is assumed to be stationary and in thermal equilibrium with the surroundings. The transient process starts by switching the heater on ( $t > 0$ ). The gas is assumed to be incompressible, viscous, heat conducting and obedient to the ideal gas laws. The relevant physical properties of the gas are thermal conductivity ( $k$ ), dynamic viscosity ( $\mu$ ), and specific heat capacity ( $C_p$ ).

Due to the complex nature of the model domain, the actual design of the heater is not taken into account in this model's equations. The heater aspect of this simulation was simplified by considering a volumetric heat source in the region where the downhole heater is located.

With the Boussinesq approximation assumed, the fluid motion and energy transport in the tube and annulus are governed by the axisymmetric, time-dependent turbulent Navier-Stokes equations and energy equation, respectively. Referring to a cylindrical coordinate frame ( $x, r$ ) with corresponding velocity components ( $U, V$ ), these equations are as follows, using standard notation:

Continuity

$$\frac{\partial(\rho U)}{\partial x} + \frac{1}{r} \frac{\partial(r\rho V)}{\partial r} = 0 \dots \dots \dots (4)$$

Momentum Equations

Axial momentum equation ( $U_D$ -momentum equation)

$$\frac{\partial(\rho U)}{\partial t} + \frac{\partial(\rho U U)}{\partial x} + \frac{1}{r} \frac{\partial(r\rho V U)}{\partial r} = -\frac{\partial P}{\partial x} - g\beta\rho(T - T_r) + \mu_a \left[ \frac{\partial^2 U}{\partial x^2} + \frac{1}{r} \frac{\partial}{\partial r} \left( r \frac{\partial U}{\partial r} \right) \right] \dots \dots (5)$$

Radial momentum equation ( $V_D$ -momentum equation)

$$\frac{\partial(\rho V)}{\partial t} + \frac{\partial(\rho U V)}{\partial x} + \frac{1}{r} \frac{\partial(r\rho V V)}{\partial r} = -\frac{\partial P}{\partial r} + \mu_a \left[ \frac{\partial^2 V}{\partial x^2} + \frac{1}{r} \frac{\partial}{\partial r} \left( r \frac{\partial V}{\partial r} \right) - \frac{V}{r^2} \right] \dots \dots \dots (6)$$

Energy Equation

$$\frac{\partial(\rho C_p T)}{\partial t} + \frac{\partial(\rho C_p U T)}{\partial x} + \frac{1}{r} \frac{\partial(r\rho C_p V T)}{\partial r} = k_a \left[ \frac{\partial^2 T}{\partial x^2} + \frac{1}{r} \frac{\partial}{\partial r} \left( r \frac{\partial T}{\partial r} \right) \right] + Q \dots \dots \dots (7)$$

In Equation (5), the second term on the left hand side is the buoyancy term and the quantity  $Q$  in Equation (7) is the volumetric heat source. The value of  $Q$  is zero, except in the heater region, where a volumetric fraction of total heat is assigned.

The flow of gas through the perforated casing, perforated cement, damaged zone and formation is assumed to be governed by the non-Darcy flow equation. Specifically, the Brinkmann extended non-Darcy model (Chan et. al., 1991; Mishima and Szekely, 1989) is used to incorporate the viscous effect of the gas in the near wellbore region where fluid velocities are high. In modelling the flow in this region, the following assumptions are made:

- the porous medium is considered as a continuum,
- the gas and the porous matrix are in local thermal equilibrium,
- the effect of natural convection is taken into account through the Boussinesq approximation.

With the above assumptions, the general macroscopic conservation equations for mass, momentum and heat transfer applicable below the overburden and through the casing, cement, damaged zone and formation can be written as follows:

Continuity

$$\frac{\partial(\rho U_D)}{\partial x} + \frac{1}{r} \frac{\partial(r\rho V_D)}{\partial r} = 0 \dots \dots \dots (8)$$

Momentum Equations

Axial momentum equation ( $U_D$ -momentum equation)

$$\frac{\partial(\rho U_D)}{\partial t} = -\frac{\partial P_D}{\partial x} - g\beta\rho\phi(T - T_r) + \mu_a \left[ \frac{\partial^2 U_D}{\partial x^2} + \frac{1}{r} \frac{\partial}{\partial r} \left( r \frac{\partial U_D}{\partial r} \right) \right] - \frac{\mu_a \phi U_D}{K} \dots \dots \dots (9)$$

Radial momentum equation ( $V_D$ -momentum equation)

$$\frac{\partial(\rho V_D)}{\partial t} = -\frac{\partial P_D}{\partial r} + \mu_a \left[ \frac{\partial^2 V_D}{\partial x^2} + \frac{1}{r} \frac{\partial}{\partial r} \left( r \frac{\partial V_D}{\partial r} \right) - \frac{V_D}{r^2} \right] - \frac{\mu_a \phi V_D}{K} \dots \dots (10)$$

Energy Equation

$$\frac{\partial \left[ (\rho C_p)_f \phi + (\rho C_p)_s (1 - \phi) \right] T}{\partial t} + \frac{\partial \left[ (\rho C_p)_f U_D T \right]}{\partial x} + \frac{1}{r} \frac{\partial \left[ r (\rho C_p)_f V_D T \right]}{\partial r} = k_e \left[ \frac{\partial^2 T}{\partial x^2} + \frac{1}{r} \frac{\partial}{\partial r} \left( r \frac{\partial T}{\partial r} \right) \right] \dots (11)$$

where  $U_D$  and  $V_D$  are the volume-averaged (Darcian) velocities in the axial and radial directions, respectively;  $P_D$  is the volume averaged pressure;  $(\rho C_p)_f$  and  $(\rho C_p)_s$  are the volumetric heat capacities of the fluid and solid, respectively;  $k$  is the permeability of the porous medium;  $k_e [k_a \phi + k_s (1 - \phi)]$

is the effective thermal conductivity;  $k_a$  is the thermal conductivity of the fluid in the porous medium;  $\phi$  is the porosity of the porous medium. Because of radial symmetry, only one half of the domain shown in Figure 2 has been considered.

The above general equations for a porous medium have been modified to account for the flow through the perforated casing and cement, damaged and formation zones.

### Initial Conditions

The initial conditions are:

$$U = V = 0 \text{ (at } t = 0) \dots\dots\dots (12)$$

$$T(t = 0, x, r) = T(t = 0, x = 0, r) + a \times x \dots\dots\dots (13)$$

$$P(t = 0, x = 0, r) = P_i \dots\dots\dots (14)$$

where  $a$  is the geothermal temperature gradient;  $x$  is the axial distance from the top of the lower segment;  $P_i$  is the average inlet pressure in the tubing or annulus.

### Boundary Conditions

At  $T > 0$ , the boundary conditions are:

$$\text{at } r = 0, \frac{\partial U}{\partial r} = V = \frac{\partial T}{\partial r} = 0 \dots\dots\dots (15)$$

$$\text{at } x = XL, U = V = 0, -k_a \frac{\partial T}{\partial x} = h_3(T - T_{x=XL}) \dots (16)$$

$$\begin{aligned} \text{at } r = YL, 0 < x < (XL - h), U = V = 0, -k_b \frac{\partial T}{\partial r} \\ = h_1(T - T_x) \dots\dots\dots (17) \end{aligned}$$

$$\begin{aligned} \text{at } r = YL, (XL - h) < x < XL, U = 0, \frac{\partial V}{\partial r} = 0, \\ -k_a \frac{\partial T}{\partial r} = h_2(T - T_x) \dots\dots\dots (18) \end{aligned}$$

$$\text{at } x = 0, 0 < r < d_{ii}/2, U = U_i, V = 0, T = T_i \dots\dots (19)$$

$$\text{at } x = 0, d_{io}/2 < r < d_{ci}/2, U = U_i, V = 0, T = T_i \dots (20)$$

where  $h_1, h_2, h_3$ , and  $h_4$  are the equivalent convective heat transfer coefficients at the formation, overburden, underburden and top of the overburden, respectively;  $h$  is the height of the formation (net pay);  $XL$  and  $YL$  are the vertical height and radial depth of the computational domain;  $d_{ii}, d_{io}$  and  $d_{ci}$  are inner diameter of the tube, outer diameter of the tube and inner diameter of the casing, respectively;  $k_b$  is the thermal conductivity of the overburden.

### Numerical procedure

The dimensional form of the above sets of elliptic partial differential equations was solved numerically by a control volume finite difference scheme. The lower segment, incorporating a part of the overburden and the formation, constitutes the full computational domain. The governing transport equations for the fluid, solid and porous regions were

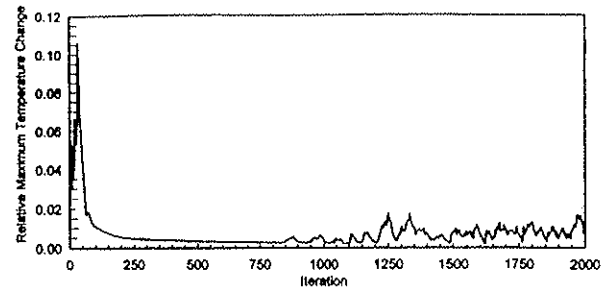


Figure 3 — Convergence of maximum relative temperature change.

solved simultaneously as a single domain problem. The finite-difference equations were derived by integrating the differential equations over an elementary control volume surrounding a grid node appropriate for each dependent variable (Patankar, 1980). A staggered grid system was used so that the scalar properties,  $P$  and  $T$ , were stored midway between the  $U$  and  $V$  velocity grid nodes (Patankar, 1980). A power-law scheme (Patankar, 1980) was used for the convective terms, and the integrated source terms were linearized. The pressure-velocity coupling of the momentum equations was resolved using the popular SIMPLER algorithm (Patankar, 1980). The governing finite-difference equations were solved iteratively by the tri-diagonal matrix algorithm (TDMA) and using a bloc-correction scheme with under-relaxation until the solutions converged.

Simulations were performed using non-uniform grids in both axial and radial directions. A non-uniform matrix of 80 by 80 nodes was used in the simulation. In the axial direction, the first 7 metres from the bottom of the reservoir was divided into 0.1 m layers. The next 3 m distance was divided into 0.5 m layers and the remaining 10 m distance at the top of the model domain was divided into 2.5 m layers. In the radial direction, the first 0.085 m was divided into 0.005 m steps and the remaining distance was divided into 0.078 m steps. The use of non-uniform grids in the radial direction was crucial because of relative dimension of the wellbore (casing diameter = 0.11 m), which is extremely small compared to the radial extension of the model domain (5 m). The non-uniform grid in the axial and radial directions was suitably placed to accommodate the various interfacial boundaries. The axial grid distance was chosen to accommodate the heater region. The solutions were to be converged, when the following criterion was satisfied simultaneously by each computed variable:

$$\text{Max} \frac{|\phi_{i,j}^{n+1} - \phi_{i,j}^n|}{|\phi_{i,j}^{n+1}|} < 0.001 \dots\dots\dots (21)$$

where  $\phi_{i,j}$  represents any dependent variable and  $(n + 1)$  refers to the value of  $Q_{i,j}$  at the  $(n + 1)$ th iteration level. To reduce computing time, the convergence criterion was monitored and it was identified that the relative difference between the parameter values of two consecutive iterations were within 0.001 after 700 to 800 iterations. As an example, the relative changes in temperature values are plotted in Figure 3. As seen in the figure, the relative changes in parameter values start to fluctuate after 800 iterations. The temperature values calculated using engineering approximation ( $mC_p\Delta T$ ) match very well with the average of the simulated temperatures of the exit gas after 800 iterations. Therefore, all simulation runs were terminated after 800 iterations.

TABLE I  
Parameters Used in the Simulation Runs

Parameters	Values
Reservoir, overburden and underburden characteristics	
Reservoir depth from surface (m)	1500
Net pay (m)	5
Porosity	15
Damaged zone permeability (mD)	5
Reservoir permeability (mD)	25
Heat loss coefficient for over/under burden ( $W/m^2 \cdot K$ )	2.5
Heat loss coefficient for reservoir ( $W/m^2 \cdot K$ )	3.0
Reservoir temperature ( $^{\circ}C$ )	52
Relevant dimensions of well, cement and damaged zone	
Inner radius of the heater (m)	0.04
Outer radius of the heater (m)	0.045
Inner radius of the casing (m)	0.055
Outer radius of the casing (m)	0.065
Outer radius of cement (m)	0.085
Outer radius of damaged zone (m)	0.961
Outer radius of formation (m)	5.0
Nitrogen characteristics	
Kinematic viscosity ( $m \cdot s$ )	$30 \times 10^{-5}$
Specific heat ( $J/kg \cdot ^{\circ}C$ )	1090
Thermal conductivity ( $W/m \cdot K$ )	0.0516
Equivalent Convective Heat Transfer Coefficients ( $W/m^2 \cdot K$ )	
$h_1$ : Heat transfer coefficient for formation	3.0
$h_2$ : Heat transfer coefficient for overburden	2.5
$h_3$ : Heat transfer coefficient for underburden	2.5
$h_4$ : Heat transfer coefficient for top of domain surface	2.0

Note: Other thermal properties of the reservoir, overburden and underburden are taken from Butler (1991).

The model was originally developed for transient solutions of the transport equations. The transient solution to the governing equations uses a fully implicit scheme. Omission of transient terms from the model equations resulted in steady state solutions. In this paper, results related to steady state solutions of the modelled equations are presented along with a brief discussion of the transient solutions.

## Results and discussion

### TRANSIENT SOLUTIONS

Transient solutions of the partial differential equations describing the mass, momentum and energy of the gas injected down the tubing and annulus were carried out. It was assumed that at every instant the gas, surrounding perforated casing, cement and porous formation were in a thermal equilibrium condition (i.e. there was no thermal dispersion effect). Also, it was initially assumed that gas in the wellbore and the formation were at a temperature given by the (constant) ambient surface temperature plus the product of depth and geothermal gradient (assumed to be constant).

Transient calculations at full power input to the tool revealed that within 30 minutes, the near wellbore region reached a thermal equilibrium condition. This short time required to reach a steady state was due to heating a confined region resulting in low heat losses (about 5%) to the unproductive strata above and below the formation. Initially, when the heater was turned on, the temperature difference between the gas and the surrounding near-wellbore

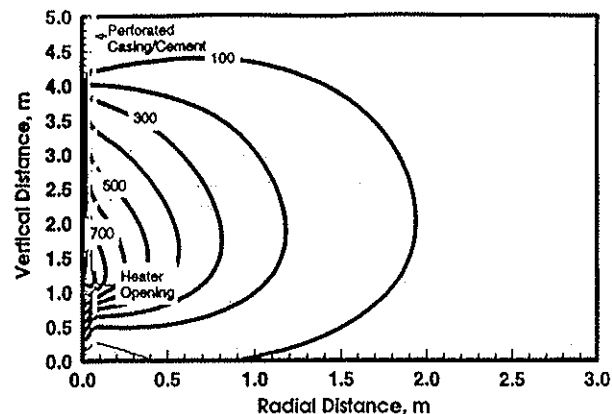


Figure 4 — An example temperature contour plot (Run #B) (power: 55 kW; flow  $4 m^3(STP)/min$ ; tubing flow fraction: 90%). The values shown for the contours are temperatures, in  $^{\circ}C$ .

region was large, resulting in a high rate of conductive and convective heat transfer. As a result, the temperature adjacent to the wellbore rose quickly. Because the segments of the casing, cement and formation adjacent to the heater largely controlled the heat transfer rate, the temperature therefore became constant when these segments approached thermal equilibrium. Convective heat transfer through these porous segments played a significant role in the attainment of thermal equilibrium in a short time. Therefore, subsequent analyses concentrated on the steady-state solution of these equations.

### STEADY STATE SOLUTIONS

The parameters used in these simulation runs are presented in Table 1. Simulation conditions, average temperatures of the exit gas and average temperatures at a radial distance of 0.5 m into the reservoir are tabulated in Table 2. The results are presented graphically in Figures 4 through 8.

To understand the practical feasibility of the FHT process and to identify the critical parameters affecting this down-hole heating process, various simulation runs were carried out. During the simulation runs, the controllable critical parameters, such as nitrogen flow rate and total power requirement at the heater were varied. The effects of these changes under steady state conditions on the temperature of the gas leaving the heater, depth of heat penetration into the reservoir and the temperature distribution in the near-wellbore region were studied and the results are presented in this paper. Based on these parametric studies, conditions were selected for field testing of the tool and the FHT process.

An example temperature contour plot is presented in Figure 4 (Run B, Table 2). As seen in this figure, the highest temperature is seen to be concentrated around the hot region of the heater (1 to 4 m). As expected, the temperature gradually decreases radially to the reservoir temperature. There are no apparent changes in the temperature due to permeability variation from damaged zone (5 mD extending to 1 m) to the rest of the reservoir (25 mD). This is possibly because of low velocity of nitrogen gas in the porous medium. Under pressure the hot nitrogen gas, exiting the heater, enters through the perforated casing and cement and travels into the porous reservoir. Gas flow into the region below the heater within the wellbore and up the annular space is minimal as the only exit is through the porous formation.

TABLE 2  
Summary of Conditions Used in These Simulation Runs and Selective Results

Runs	Total Power (kW)	Total Flow [m <sup>3</sup> (STP)/min]	Flow Fraction in Tubing (%)	Average Exit Gas Temperature (°C)		Temperature at 0.5 m from the Centre of the Wellbore (°C)	
				Simulation	Engineering Calculation*	Maximum	Average Over Vertical Distance of 5 m Net Pay
A	55	2	90	1070	1417	339	215
B	55	4	90	761	735	421	262
C	55	4	80	780	820	425	261
D	55	6	90	644	507	445	294
E	55	10	90	409	325	384	295
F	80	4	90	1239	1045	565	346
G	40	4	90	567	548	330	210
H (field test)**	34	5.5	70	473	446	319	201

\* Engineering calculations were carried out using  $mC_p \Delta T$  relations (flow going through the tube is assumed to pick up all heat).  
\*\* Measured temperature during field test (non steady state): 382°C

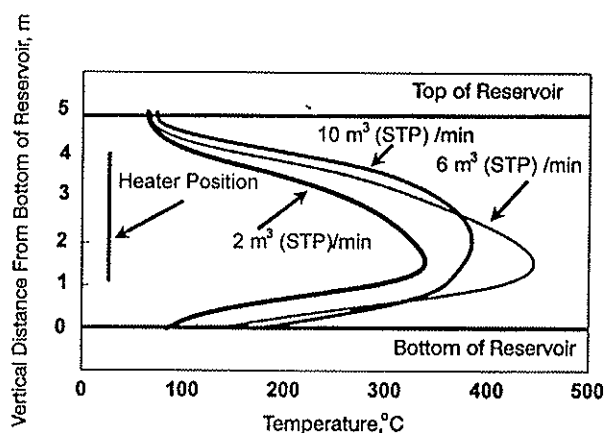


Figure 5 — Temperature profile at 0.5 m from the centre of the wellbore as a function of nitrogen flow rate (Heater power: 55 kW; 90% flow through the tubing).

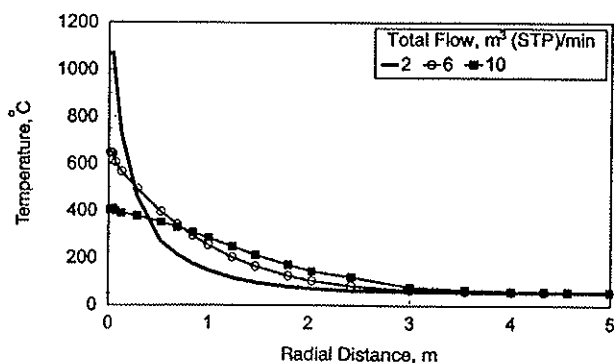


Figure 6 — Temperature profile in the radial direction as a function of total flow rate at 1.1 m from the bottom of the model domain (Heater power: 55 kW; 90% flow through the tubing).

The effect of the total volumetric flow rate, m<sup>3</sup>(STP)/min, on the vertical temperature distribution at a fixed radial distance of 0.5 m is presented in Figure 5. In these cases, the heater power was 55 kW with a tubing flow fraction of 90% and the heater was placed at 1 m from the bottom of the

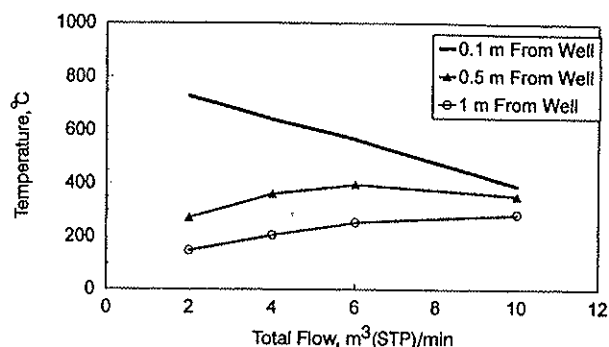


Figure 7 — Temperature as a function of total flow at 1.1 m from the bottom of the model domain (Heater power: 55 kW; 90% flow through the tubing).

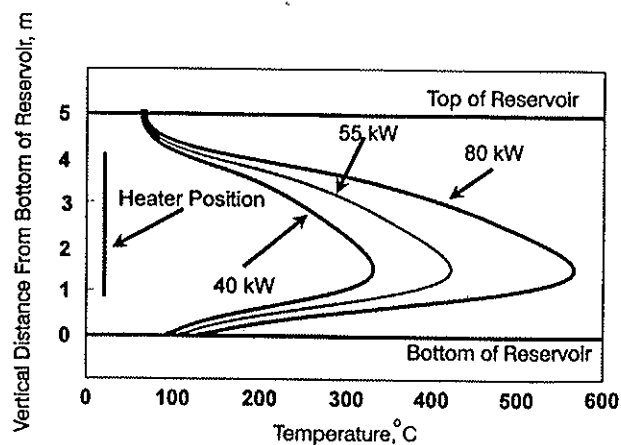


Figure 8 — Temperature profile at 0.5 m from the centre of the wellbore as a function of heater power (Total flow 4 m<sup>3</sup>(STP)/min and 90% is through the tubing).

model domain. As seen in the figure, temperature increases and reaches a maxima within the flow rates of about 2 to 10 m<sup>3</sup>(STP)/min. As expected, in all situations, the maximum temperature is at the heater openings from where the hot gas exits the heater. The vertical temperature profile is also seen

to be more rounded for a flow rate of  $10 \text{ m}^3(\text{STP})/\text{min}$  indicating a greater vertical dispersion of hot gas. Although the highest temperature at a  $0.5 \text{ m}$  radial distance is achieved at a flow rate of  $6 \text{ m}^3(\text{STP})/\text{min}$ , the average temperature over the vertical distance is seen to be almost the same for these two cases (Runs D and E in Table 2).

The temperature profile in the radial direction at a fixed vertical location of  $1.1 \text{ m}$  from the bottom of the model domain is presented in Figure 6 as a function of total flow rate. As expected, the increase in flow rate results in a lower temperature of the gas exiting the heater because of fixed heater power ( $55 \text{ kW}$ ). It is important to note that the higher exit gas temperature will not necessarily provide higher heat penetration into the near wellbore region. Fluid velocity in the porous medium will play an important role in achieving a higher temperature at various radial distances. At a low flow rate,  $2 \text{ m}^3(\text{STP})/\text{min}$ , the temperature in the near wellbore region (within  $0.1 \text{ m}$ ) is very high ( $> 1000^\circ\text{C}$ ). However, this temperature quickly drops off to less than  $200^\circ\text{C}$  at a radial distance of  $1 \text{ m}$ . This is an indication of conduction dominated heat transfer mechanism. Low flow rate will result in high temperature, however, the velocity related to low flow rate is so small that heat penetration in the porous medium will also be small (Figure 6). On the other hand, at a high flow rate,  $10 \text{ m}^3(\text{STP})/\text{min}$ , the exit gas temperature is low ( $400^\circ\text{C}$ ), but the temperature at a radial distance of  $1 \text{ m}$  is around  $300^\circ\text{C}$ . This is an indication of convection dominated heat transfer mechanism. Since the power is limited to  $55 \text{ kW}$ , a flow rate in the range of  $4$  to  $10 \text{ m}^3(\text{STP})/\text{min}$  will provide a temperature greater than  $300^\circ\text{C}$  within the target radial distance of  $1 \text{ m}$ .

The maximum temperature at a specific radial distance is dependent on the gas flow rate. If one wanted a high near wellbore temperature, a low flow rate is recommended. However, if a greater heat penetration into the formation is required, then a higher flow rate will be needed. In this case, greater heat penetration will have to be compromised with a lower temperature.

Figure 7 presents temperatures as a function of flow rate at a fixed vertical location of  $1.1 \text{ m}$  from the bottom of the model domain for various radial locations. For a fixed heater power of  $55 \text{ kW}$  (Figure 7) and at a  $0.5 \text{ m}$  radial distance, the temperature reaches a maximum of  $400^\circ\text{C}$  at a flow rate of  $6 \text{ m}^3(\text{STP})/\text{min}$ . As expected, lower temperatures are achieved at a radial distance of  $1 \text{ m}$ . Close to the casing wall ( $0.1 \text{ m}$ ), however, the highest temperature is seen at the lowest flow rate,  $2 \text{ m}^3(\text{STP})/\text{min}$ . This is because the hot gas is still in the tubular region.

The variation in temperature profile at a fixed radial distance of  $0.5 \text{ m}$  for three power ratings is presented in Figure 8. These three runs were carried out at a  $4 \text{ m}^3(\text{STP})/\text{min}$  flow rate and 90% flow is flowing through the tubing. To achieve a maximum temperature of  $500^\circ\text{C}$  at  $0.5 \text{ m}$  into the reservoir, a downhole heater of at least  $80 \text{ kW}$  is required. As explained earlier, the availability of suitable power cable, voltage losses in the cable ( $\geq 1500 \text{ m}$  long) and internal diameter of the well casing limits the practicality of using higher power in a resistive type heating device.

To study the effect of variation in the tubing flow fraction on the attainable temperature at a radial distance of  $0.5 \text{ m}$  from the centre of the wellbore, two cases were studied. Variations in the tubing flow fraction of 80% and 90% did not have significant impact on the average temperature at a radial distance of  $0.5 \text{ m}$  (Table 2).

To evaluate the efficiency of the stimulation process, an overall heat balance was carried out for the near wellbore region. At a steady state, the heat dissipated by the heater equals the heat losses in the over and underburden and heat gain in the reservoir. The heat loss calculations using  $55 \text{ kW}$  power, a total flow of  $4 \text{ m}^3(\text{STP})/\text{min}$ , flow through the tubing indicated that less than 5% of the  $55 \text{ kW}$  input power was lost in the unproductive strata (overburden and underburden).

### Simulated vs measured temperature from field testing of FHT

To validate the FHT concept in the field, a proprietary resistance-type electrical heater was developed to conduct the heating process downhole. The heater was successfully tested at the surface several times and subsequently, the heater was tested in the field (Jamaluddin et al., 1996a). To avoid the risks of damaging the wellbore casing due to thermal shock in a producing well, a depleted well slated for abandonment was chosen. During the field test, the heater was lowered into the target reservoir  $1.5 \text{ km}$  downhole, heated up to a temperature of  $382^\circ\text{C}$ , and retrieved from the wellbore.

The total nitrogen flow was maintained at  $5.5 \text{ m}^3(\text{STP})/\text{min}$ ,  $4 \text{ m}^3(\text{STP})/\text{min}$  in the tubing and  $1.5 \text{ m}^3(\text{STP})/\text{min}$  in the annulus. The injection pressure was stabilized at  $3.7 \text{ MPa}$ . The heater was slowly powered up to achieve a target exit gas temperature of  $700^\circ\text{C}$ . This target temperature was designed corresponding to  $5.5 \text{ m}^3(\text{STP})/\text{min}$  and a power input of  $55 \text{ kW}$ . However, the heater failed within 1 minute of achieving an input power of  $34 \text{ kW}$  at the heater. The heater failure occurred due to an electrical short circuit caused by water leakage into the junction box. At the instant of failure, the measured temperature of the gas exiting the heater at downhole conditions was  $382^\circ\text{C}$ . The thermocouple was located at the bottom end of the heater as shown in Figure 2. An engineering calculation based on 70% nitrogen flowing through the heater would correspond to  $446^\circ\text{C}$  of the exit gas at steady state conditions. Simulation results indicate that at a steady state condition corresponding to a total nitrogen flow of  $5.5 \text{ m}^3(\text{STP})/\text{min}$  and at a power input of  $34 \text{ kW}$ , the exit gas temperature would be  $473^\circ\text{C}$ . Correspondingly, this exit gas would have resulted in an average temperature of  $200^\circ\text{C}$  at a radial distance of  $0.5 \text{ m}$  into the reservoir.

As presented in the earlier paper (Jamaluddin et al., 1996a), the target field test objective of raising the downhole temperature to  $+700^\circ\text{C}$  was not satisfied due to the heater failure, but the most important aspect of the effect of heat on the reservoir characteristics was estimated using type curve matching technique. The permeability of the near wellbore reservoir was improved six fold, which has enormous potential benefits for hydrocarbon producing wells.

### Concluding remarks

The mathematical model presented in this paper demonstrates the feasibility of the formation heat treatment process using a downhole resistance-type electrical heater. The heat is conveyed to the near-wellbore region by nitrogen gas passing through the heater located downhole by means of conduction and convection. Transient solutions of the modeled equations have shown that when initially both the gas in the wellbore and the reservoir are in equilibrium with the

geothermal temperature profile, the time required for the near wellbore region (confined region) to reach thermal equilibrium is less than 30 minutes. Results show that for a volumetric gas flow rate of 6 m<sup>3</sup>(STP)/min and a heater power of 55 kW a temperature of 400°C can be attained at a radial distance of 0.5 m in the reservoir. Simulation results indicate that to achieve a higher temperature at 0.5 m in the reservoir, a higher-power heating system is required. Calculations have revealed that the total heat loss to the unproductive strata above and below the formation is less than 5% of the power rating of the heater.

### Acknowledgements

The authors wish to thank Noranda Inc. and Norcen Energy Resources Limited for the permission to publish this work.

### Nomenclature

$a$	— geothermal temperature gradient, °C/m
$d$	— diameter of the tube or the equivalent diameter of the annulus, m
$d_{ji}$	— inner diameter of the tube, m
$d_{to}$	— outer diameter of the tube, m
$d_{ci}$	— inner diameter of the casing, m
$D$	— diameter of the tube, m
$f$	— turbulent friction factor
$h$	— height of the formation (net pay), m
$h_1$	— equivalent convective heat transfer coefficients at the formaion, W/m <sup>2</sup> •K
$h_2$	— equivalent convective heat transfer coefficients at overburden, W/m <sup>2</sup> •K
$h_3$	— equivalent convective heat transfer coefficients at underburden, W/m <sup>2</sup> •K
$h_4$	— equivalent convective heat transfer coefficients at the top of the overburden, W/m <sup>2</sup> •K
$H$	— total height of the tube, m
$k$	— permeability of the porous medium, mD
$k_b$	— thermal conductivity of the overburden, W/m•K
$k_e$	— effective thermal conductivity, W/m•K
$k_a$	— thermal conductivity of the fluid in the porous medium, W/m•K
$P_D$	— volume averaged pressure, kPa
$P_i$	— average inlet pressure in the tubing or annulus, kPa
$P_{wf}$	— pressure in the tubing annulus, kPa
$P_f$	— pressure at the inlet of the tube or annulus, kPa
$q$	— total volumetric gas flow rate through the tube or annulus, m <sup>3</sup> (STP)/min
$Q$	— volumetric heat source, W/m <sup>3</sup>
$Re$	— Reynolds number for the tube or annulus, $Re = \rho v D / \mu$
$T_{ag}$	— average geothermal temperature, °C
$v$	— velocity of fluid, m/sec
$U_D$	— volume averaged (Darcian) velocities in the axial direction, m/sec
$V_D$	— volume averaged (Darcian) velocities in the radial direction, m/sec
$x$	— axial distance from the top of the lower segment, m
$XL$	— vertical height of the computational domain, m
$YL$	— radial depth of the computational domain, m
$Z$	— gas compressibility factor

### Greek letters

$\gamma_g$	— specific gravity of the gas
$\epsilon$	— roughness in the tube or the tube casing annulus
$\mu$	— fluid viscosity, mPa.s
$\rho$	— fluid density, kg/m <sup>3</sup>
$(\rho C_p)_f$	— volumetric heat capacity of the fluid, J/m <sup>3</sup> •°C
$(\rho C_p)_s$	— volumetric heat capacity of the solid, J/m <sup>3</sup> •°C
$\phi$	— porosity of the porous medium
$\varphi$	— represents any dependent variable

### References

- Albaugh, F. W., "Oil Well Production Process", U.S. Patent 2,685,930 (1954).
- Beggs, H. D., "Gas Production Operations", OGCI Publications, Tulsa, OK (1984), pp. 96–104.
- Borchardt, J. K., D. L. Roll and L. M. Rayne, "Use of a Mineral-Fines Stabilizer in Well Completions", paper presented at the California Regional Meeting of the Society of Petroleum Engineers, Long Beach, CA, April 11–13 (1984).
- Braun, P. H., "Method for Increasing Subterranean Formation Permeability", U.S. Patent 3,603,396 (1971).
- Butler, R. M., "Thermal Recovery of Oil and Bitumen", Prentice Hall, Englewood Cliffs, NJ (1991).
- Carcoana, A., "Applied Enhanced Oil Recovery", Prentice Hall, Englewood Cliffs, NJ (1992), pp. 122–127.
- Carroll, D., "Clay Minerals: A Guide to Their X-ray Identification", The Geological Society of America, Menlo Park, CA, special issue 126 (1970).
- Chan, K. S., K. Pericleous and M. Cross, "Numerical Simulation of Flows Encountered During Mold Filling", Appl. Math. Modelling 15, 624–631 (1991).
- Coppell, C. P., H. Y. Jennings and M. G. Reed, "Field Results from Wells Treated with Hydroxy-Aluminum", J. Petrol. Tech., 1108–1112 (September 1973).
- Crowe, C. W., "Precipitation of Hydrated Silica from Spent Hydrofluoric Acid — How Much of a Problem is it?", J. Petrol. Tech. (November, 1986).
- Friedman, R. H., B. W. Surles, and D. E. Kleke, "High Temperature Sand Consolidation", Soc. Petrol. Eng. Production Eng. J., 167–172, (May 1988).
- Garst, A. W., "Increasing the Permeability of Earthy Formations", U.S. Patent 2,782,859 (1957).
- Hayatdavoudi, A., A. Bailey, R. Ehrlich and A. Ghalambor, "Applied Clay Engineering: Formation Damage Aspects of Clays", Short Course, SPE Formation Damage Symposium, Lafayette, LA (1992).
- Himes, R. E., E. F. Vinson and D. E. Simon, "Clay Stabilization in Low-Permeability Formations", Soc. Petrol. Eng. Prod. Eng. J., 252–258 (August, 1991).
- Hoang, V., "Estimation of *In-situ* Thermal Conductivities from Temperature Gradient Measurements", Ph.D. Dissertation, Univ. of California, Berkeley (1980).
- Jamaluddin, A. K. M. and T. W. Nazarko, "Process for Increasing Near-Wellbore Permeability of Porous Formations", U.S. Patent 5,361,845 (1994).
- Jamaluddin, A. K. M., L. M. Vandamme, T. W. Nazarko and D. B. Bension, "Heat Treatment for Clay-Related Near Wellbore Formation Damage", paper CIM 95–67 presented at the 46<sup>th</sup> Annual Technical Meeting of the Petroleum Society of CIM in Banff, Alberta, Canada, May 14–17 (1995).
- Jamaluddin, A. K. M., M. Hamelin, K. Harke, H. McCaskill and S.A. Mehta, "Field Testing of the Formation Heat Treatment", paper CIM 96–88 presented at the 47<sup>th</sup> Annual Technical Meeting of the Petroleum Society of CIM in Calgary, Alberta, Canada, June 10–12 (1996a).
- Jamaluddin, A. K. M., S. A. Mehta, R. G. Moore and R. G. McGuffin, "Downhole Heating System with Separate Wiring, Cooling, and Heating Chamber, and Gas Flow Through", U.S. Patent 5,539,853 (1996b).
- Lund, L., H. S. Fogler and C. C. McCune, "Predicting the Flow and Reaction of HCl/HF Acid Mixtures in Porous Sandstone Cores", Soc. Petrol. Engg. J., Trans. AIME 261, 248–260 (1976).
- Mishima, S. and J. Szekely, "The Modelling of Fluid Flow and Heat Transfer in Mold Filling", ISIJ International 29, 324–332 (1989).
- Nenniger, J. E., "Method and Apparatus for Oil Well Stimulation Utilizing Electrically Heated Solvents", U.S. Patent 5,120,935 (1992).
- Nooner, D. W., "Reservoir Stabilization by Treating Water-Sensitive Clays", U.S. Patent 4,227,575 (1980).

- Patankar, S. V., "Numerical Heat Transfer and Fluid Flow", Hemisphere, Washington, DC (1980).
- Plummer, M. A., "Preventing Plugging by Insoluble Salts in a Hydrocarbon-Bearing Formation and Associated Production Wells", Canadian Patent 1,282,685 (April, 1991).
- Ramey, H. J. Jr., "Wellbore Heat Transmission", *J. Petrol. Technol.* 427-434 (April, 1962).
- Reed, M. G., "Formation Permeability Maintenance with Hydroxy-Aluminum Solutions", U.S. Patent 3,827,500 (1974).
- Reed, M. G., "Permeability of Fines-Containing Earth Formations by Removing Liquid Water", U.S. Patent 5,052,490 (1991a).
- Reed, M. G., "Method of Improving Permeability of Fines-Containing Hydrocarbon Formations by Steam Injection", U.S. Patent 5,058,681 (1991b).
- Schaible, D. F., "Identification, Evaluation, and Treatment of Formation Damage, Offshore Louisiana", paper presented at the Seventh Society of Petroleum Engineering Symposium on Formation Damage Control, Lafayette, LA, February 26-27 (1986).
- Sharma, Y., O. Shoham and J. P. Brill, "Simulation of Downhole Heater Phenomena in the Production of Wellbore Fluids", *Soc. Petrol. Eng. Production Eng. J.*, 309-312 (August, 1989).
- Sloat, B. F., "Nitrogen Stimulation of a Potassium Hydroxide Wellbore Treatment", U.S. Patent 4,844,169 (1989).
- Somerton, W. H., "Thermal Properties and Temperature Related Behaviour of Rock/Fluid Systems, Elsevier, New York (1992), pp. 215-222.
- Theng, B. K. G., "The Chemistry of Clay-Organic Reactions", Halsted Press Div., John Wiley & Sons, New York (1984).
- Thomas, R. L. and C. W. Crowe, "Matrix Treatment Employs New Acid System for Stimulation and Control of Fines Migration in Sandstone Formations", *J. Petrol. Technol.*, 1491-1500 (August, 1981).
- White, P. D. and J. T. Mass, "High Temperature Thermal Techniques for Stimulating Oil Recovery", *J. Petrol. Technol.*, 1007-1015 (September, 1965).
- Winckler, E. and J. W. McManus, "Method and Apparatus for Removal of Oil Well Paraffin", U.S. Patent 4,911,239 (1990).

---

Manuscript received May 28, 1996; revised manuscript received February 21, 1997; accepted for publication March 12, 1997.